Food Hydrocolloids 171 (2026) 111807

Contents lists available at ScienceDirect

Food Hydrocolloids

journal homepage: www.elsevier.com/locate/foodhyd

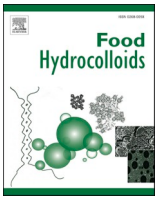

Emulsion gels of oil encapsulated in double polysaccharide networks as animal fat analogues

Yong Wang [a,1], Canice Chun-Yin Yiu [a,1], Woojeong Kim [a], Jitraporn Vongsvivut [b], Weibiao Zhou [c], Cordelia Selomulya [a,*]

[a] School of Chemical Engineering, UNSW Sydney, NSW, 2052, Australia
[b] Infrared Microspectroscopy (IRM) Beamline, ANSTO – Australian Synchrotron, 800 Blackburn Road, Clayton, VIC, 3168, Australia
[c] Department of Food Science and Technology, National University of Singapore, Singapore, 117542, Singapore

ARTICLE INFO

Keywords:
Curdlan gum
Pea protein
Emulsion gel
Konjac glucomannan
Fat analogue
Synchrotron infrared microspectroscopy

ABSTRACT

The development of plant-based alternatives to replace animal products is crucial as the global population nears 10 billion by 2050, necessitating more sustainable food systems. Although efforts has been made in mimicking animal muscle textures using plant-based proteins, particularly the texturized plant proteins, the replication of animal fat properties remains challenging and less explored, particularly in light of recent commercial setbacks in the plant-based meat industry. Current study addressed this gap by investigating curdlan gum-konjac glucomannan (KGM)-pea protein emulsion gels as fat analogues, focusing on their stability and structure formation during cooking. We found that the use of a double polysaccharide network significantly enhanced the stability of emulsion gels, both before and after thermal processing, with controlled thermal history effectively guiding the gel morphology. Pea-protein-stabilised canola-oil emulsions (oil: 10–40 % w/w; protein: 5 % w/w) were blended with hydrated curdlan/KGM dispersions (total 4–7 %, w/w) and thermally set through a two-step heating regime (50 °C for 15 min, then 85 °C for 30 min) to form emulsion gels. Gels containing 6 % polysaccharide and 30 % oil exhibited only 57 ± 5 % oven shrinkage (pork fat = 63 ± 12 %), <15 % oil/water loss after five freeze-thaw cycles, and springness of 0.42 ± 0.05 (pork fat = 0.48 ± 0.06). Synchrotron-FTIR chemical imaging data confirmed the role of protein and polysaccharides in maintaining structural integrity, aligning with visual and rheological analyses. For the first time, we demonstrate that a sequentially gelled curdlan–KGM double network, reinforced by pea-protein interfaces, can lock sizable amounts of unsaturated oil into a cohesive matrix that reproduces the shrinkage, browning, and oil release of animal fat during cooking. This work therefore establishes a new, thermo-responsive route to plant-based fat analogues and offers mechanistic guidance for future meat-alternative formulations.

1. Introduction

Plant-based food products will play more crucial role as the global population is projected to reach 9.7 billion by 2050, according to the United Nations (Duarte et al., 2022), while the demand for food may increase by 56 % till 2050 (van Dijk et al., 2021). This anticipated growth raises concerns about the sustainability of our current food production systems, which are unlikely to meet the demands of such a large population without causing severe environmental degradation (Ray et al., 2022). To address these challenges, a transition toward more sustainable food systems is imperative, aligning with the United Nations Sustainable Development Goals (SDGs), particularly Zero Hunger (SDG 2) and Climate Action (SDG 13) (United_Nations, 2015). The rapid development of plant-based meats and cultured meat technologies has brought us closer to creating plant protein-based fibrous structures resembling animal muscle tissues (Sha & Xiong, 2020), to print the pork muscle and fat layers over each other (Guan et al., 2025), and also to 3D-printing steaks from cultured cells (Su et al., 2023). However, the majority of research has been concentrated on the protein components, leaving other crucial aspects of meat, such as fat, relatively underexplored (Cheng et al., 2024).

This article is part of a special issue entitled: 19th Food Colloids Conference published in Food Hydrocolloids.

* Corresponding author.
E-mail address: cordelia.selomulya@unsw.edu.au (C. Selomulya).

[1] These two authors contribute equally to this work.

https://doi.org/10.1016/j.foodhyd.2025.111807
Received 23 October 2024; Received in revised form 23 June 2025; Accepted 25 July 2025
Available online 26 July 2025

Abbreviations

BF	Beef fat
CUD	Curdlan
EG	Emulsion Gels
KGM	Konjac glucomannan
PF	Pork fat
PPI	Pea protein isolate
PS	Polysaccharides

High-moisture extrusion is the predominant technique for structuring plant proteins into fibrous, muscle-like matrices. Extrusion rearranges hydrated globular proteins under shear and cooling to generate the anisotropic 'lean' portion of meat analogues (Işçimen & Hayta, 2024). Because the process targets protein structuring, the extrudate contains little intrinsic lipid retention (Vallikkadan et al., 2023). Consequently, a separate fat component with comparable thermal and mechanical stability must be incorporated, either by co-extrusion or post-extrusion mixing—to mimic the marbling and succulence provided by animal adipose tissue. The design of such heat- and freeze-stable fat analogues therefore represents a complementary challenge that has received far less attention than protein texturization (Younis et al., 2023).

Moreover, fat plays a significant role in flavour release and mouthfeel, which are difficult to replicate with plant-based alternatives when using extrusion alone (Variyar & Mishra, 2024). Therefore, addressing the challenges associated with fat behaviour during processing and cooking is essential for improving the quality and consumer acceptance of plant-based meat products (Kerslake et al., 2022). A solution to address this issue in most commercial plant-based products is to use solid vegetable fat particles, such as coconut fat or palm oil/fat (Sridhar et al., 2023), which often melt rapidly during cooking including pan-frying, oven cooking, or barbecuing, resulting in an oily texture that differs markedly from the gradual fat release seen in animal fats. The sensory perception of fat remains a significant barrier in the development of plant-based meats (Sogari et al., 2023).

Although some progresses have been made in the study of fat analogues, the research in this area is still quite limited. Typically, most studies utilise a single structuring agent, such as polysaccharides or proteins, with examples including agar (Fontes-Candia et al., 2023), carrageenan (de Souza Paglarini et al., 2019), guar gum (Kamer, 2024), modified starch (Zhao et al., 2023), curdlan gum (Choi et al., 2024), konjac glucomannan (Jeong et al., 2023), and various other gums. These studies often focus on one aspect of performance, such as appearance & texture before cooking, or oil release and colour change after cooking (J. Guo, Cui, & Meng, 2023). There are some studies that use two or more structuring agents, but in most cases, they involve mixtures of ingredients aimed at producing synergistic effects on the gelation properties and stability of the food polymer networks (Xu et al., 2024), such as carrageenan & carboxymethyl dextrin (X.-L. Li, Meng, et al., 2022), agar & alginate (Choi et al., 2023), guar & xanthan (Rather et al., 2016). Oleogels have gained significant attention as an alternative to traditional fat replacers due to their ability to encapsulate oils and mimic animal fat in meat products (Martins et al., 2018). Oleogels use various oil structuring agents such as ethyl cellulose (Naeli et al., 2020) or edible waxes (Dobson & Marangoni, 2024) to create stable fat-like gels. While oleogels provide functional benefits, such as stabilizing liquid oils in structured matrices, they often face challenges such as weaker gel structures, which can lead to premature oil leakage during cooking (Gómez-Estaca et al., 2020). Additionally, their reliance on a single network structure can limit adaptability across different cooking conditions and stability at higher temperatures, which is a significant barrier for many food applications (X. Cui et al., 2023).

In contrast, we propose the use of a double polysaccharide network, a method commonly employed in materials science to build hydrogels for tissue engineering (B. Guo, Liang, & Dong, 2023) or biological 3D printing (Zhu et al., 2024). The advantage of this approach is the ability to manipulate the double polysaccharide networks to precisely control both structure formation and deformation (Nonoyama & Gong, 2021), allowing us to create structures that can mimic animal fat tissue across different stages of cooking, which to the best of our knowledge has never been reported for plant-based fat replacer. Recent attempts to structure lipid phases for meat alternatives have employed dual hydrocolloid matrices such as κ-carrageenan/locust-bean-gum, xanthan/konjac or alginate/agar; while these gels stabilize oil at room temperature, they either melt abruptly or remain rigid during cooking, producing little browning, limited shrinkage and rapid oil leakage (Choi et al., 2023; Z. Lu et al., 2025; Yang et al., 2019). By contrast, we combine the weak but flexible KGM gel with thermo-irreversible curdlan gel to fabricate a bilayer network that encapsulates canola oil (Yiu et al., 2025), then modulates visco-elasticity progressively, recreating the staged softening, browning and juiciness (as indicated by oil release) characteristic of animal fat, which were not achieved from previous studies (Huang et al., 2023; Zhou et al., 2022).

The goal of this study was to explore how non-animal ingredients could be used to effectively mimic the properties of animal fat during all stages of cooking through emulsion gel. Specifically, we used curdlan gum due to its unique ability to form both thermally reversible and thermally irreversible gels, allowing precisely controlled texture development (Wang et al., 2023). Konjac glucomannan was used for its capacity to create tough and stretchy gel structures (Z. Liu et al., 2021), with both polysaccharides forming a double network, a novel approach that had not yet been used to mimic animal fat. Curdlan undergoes a two-step thermal transition: heating to 50–60 °C yields a thermo-reversible 'low-set' gel, whereas heating above 80 °C creates a high-strength, thermo-irreversible triple-helix network that remains stable during further processing (Hirashima et al., 1997). In contrast, konjac glucomannan experiences a coil-to-helix transition near 60 °C that produces an elastic network with outstanding water-holding capacity and freeze-thaw stability (Yishen Li, Li, et al., 2024). When combined, the rapidly forming curdlan matrix immobilises oil droplets early in heating, while the more gradually setting KGM interpenetrates and reinforces the scaffold, yielding a double network that endures both oven baking and repeated freezing. This synergy, together with the carefully controlled thermal history, generates an emulsion-gel architecture not reported previously. Pea protein was used to stabilize oil emulsion and as protein inclusion for nutrient (Burger & Zhang, 2019). Additionally, we used vegetable oils rich in unsaturated fatty acids to create healthier fat profiles (Heck et al., 2022). Our approach was validated through oven cooking simulations to assess visual similarity with the changes in animal fat during cooking, confocal laser scanning microscopy (CLSM) to characterize the microstructure of the fat analogues, synchrotron-FTIR microspectroscopy to confirm our hypothesis on the structural formation mechanism, and rheological and texture profile analyses to evaluate mechanical properties. The focus here is to investigate how the combination of polysaccharides, proteins, and lipids can be used to create a versatile fat analogue, which may offer new insights for both research and industrial applications in developing fat analogues for various food products.

2. Materials and methods

2.1. Materials

Pea protein isolate (BulkNutrients®) was purchased locally (Australia), with a protein concentration of 85 % (w/w) and 5.5 % of carbohydrates (w/w). Curdlan gum powder (CAS No. 54724-00-4) was sourced from Opal Biotech (Zhengzhou, China), with a purity of 92 % (w/w) and an ash content of 3.12 % (w/w). Konjac glucomannan (KJ30

Konjac gum) was obtained from Hubei Konson Konjac Gum (Hubei Province, China), featuring an 85 % (w/w) glucomannan concentration. Canola oil, along with beef and pork fat samples, were purchased from a local supermarket in Sydney, Australia. Milli-Q water was used for all sample preparations in this study.

2.2. Emulsion gel preparation

Pea protein isolate (PPI) suspensions (5 %, w/w, in final emulsions) was prepared by rehydrating the protein in Milli-Q water and rehydrated by incubating in a thermostatic water bath at 85 °C for 30 min following a previous method (Xu et al., 2021). The PPI suspension was then combined with canola oil and mixed using an electric mixer at 750 rpm for 3 min to enhance oil incorporation before homogenizing the suspension for 3 min at 11,000 rpm using a high-shear mixer (IKA Ultra Turrax T25, Staufen, Germany). The resulting emulsion was allowed to cool to room temperature before further processing.

Once cooled, polysaccharide powders (4–7 %, w/w) were gradually incorporated into the emulsion using an electric mixer at 800 rpm. Initially, curdlan (CUD) powder was added and mixed for 3 min, followed by the addition of konjac glucomannan (KGM) powder, with mixing continued for an additional 2 min, bringing the total mixing time to 5 min. The addition of KGM helped to create viscous emulsion stock at this stage and keep the curdlan gum well dispersed in the mixture, and no visible curdlan agglomerates were observed under optical microscope. The prepared mixture was then immediately transferred into 50 mL centrifuge tubes, which were placed in a refrigerator at 4 °C and incubated overnight to ensure complete rehydration of KGM. The tubes were then subjected to a heating protocol: first to 50 °C for 15 min, followed by heating to 85 °C for 30 min using a heating block. After heating, the tubes were allowed to cool to room temperature and stored at 4 °C until further use. This procedure was applied to produce emulsion gels with varying oil, polysaccharide, and KGM content (including KGM-0 %).

Additionally, to evaluate the effect of PPI on the emulsion gels, a protein-free control emulsion, i.e. samples without PPI (designated as PPI-0 %), was prepared following a similar process, with slight modifications. In these samples, the polysaccharide blend was mixed with oil and water prior to high-shear mixing, while maintaining consistent total mixing time. The composition of each emulsion gel sample is detailed in Table 1.

For comparison, pork fat (PF) and beef fat (BF) samples were cut to match the size of the emulsion gel samples. These animal fat samples were boiled for 30 min, cooled to room temperature, and then used for textural analysis and colourimetry.

Table 1
The final formulation of samples in emulsion gels (all percentage based on w/w).

Sample	Oil (%)	Protein (%)	Polysaccharide			Water (%)
			total (%)	Curdlan (%)	KGM (%)	
Oil-10 %	10	5	6	4.8	1.2	79
Oil-20 %	20	5	6	4.8	1.2	69
Oil-30 %	30	5	6	4.8	1.2	59
Oil-40 %	40	5	6	4.8	1.2	49
PS-4 %	20	5	4	3.2	0.8	71
PS-5 %	20	5	5	4	1	70
PS-6 %[a]	20	5	6	4.8	1.2	69
PS-7 %	20	5	7	5.6	1.4	68
PPI-0 %	20	0	6	4.8	1.2	69
KGM-0 %[b]	20	5	6	6	0	74
CD-0 %[c]	20	5	6	0	6	74

[a] Sample Oil-20 % and PS-6 % are identical samples.
[b] KGM represents konjac glucomannan; CD represents curdlan gum; this sample didn't form stable gel therefore was not presented in the results.
[c] PS represents polysaccharide concentration (%).

2.3. Morphology

A confocal laser scanning microscope (CLSM, Zeiss LSM 800, Jena, Germany) was employed to observe the microstructure of the gel. Following overnight incubation at 4 °C, Nile blue A and Nile red was added to the emulsion/polysaccharide mixture to stain the PPI and oil, respectively. A small portion of the stained mixture was placed onto a microscope slide and covered with a coverslip. The slide was gently pressed to form a thin film of the pre-gelled mixture and then heated on a Peltier heater (TA Instruments ARES-G2, New Castle, USA) at 85 °C for 3 min. Micrographs were captured with a AxioCam 506 camera using 20x objective lens.

For comparative analysis of the gel appearance against animal fat, colourimetry was conducted. Emulsion gels and animal fat samples were cut into cylinders (2.5 cm in diameter and 1 cm in height) for measurement (B. Cui et al., 2022; L. Huang et al., 2022). A colourimeter (Konica Minolta CR-400, Tokyo, Japan) was used to record the objective colour CIE-LAB tristimulus value using Illuminant D65 as the detection light source. L^* (lightness), a^* (red-green axis) and b^* (blue-yellow axis) values of each emulsion gel sample and animal fat sample (cooked and raw) were recorded (B. Cui et al., 2022; L. Huang et al., 2022). The colourimeter was calibrated with a standard black plate before measurements. Ten measurements were conducted for each sample.

2.4. Freeze-thaw performance and water holding capacity

A modified procedure adapted from B. Cui et al. (2022) was used for measuring freeze-thaw stability. Twelve grams of each sample were placed in a sealed 50 mL centrifuge tube and frozen at −20 °C for 22 h. The samples were then thawed in a water bath at 30 °C for 2 h. The excess water was removed before weighing, by gently absorbing the water using filter paper. This freeze-thaw cycle was repeated five times, with measurements taken after each cycle. Each formulation was tested in triplicate, and water syneresis was calculated using Equation (1):

$$Freeze-thaw\ stability\ (\%) = \frac{A_n}{A_0} * 100\% \quad (1)$$

Where A_0 is the initial weight of the emulsion gel (g) prior to freezing, and A_n is the weight of the emulsion gel (g) after the nth freeze-thaw cycle.

Water holding capacity (WHC) is the retention of water by the gel matrix. It indicates the gel matrix's quality and textural stability (Z. Y. Zhang et al., 2015). Five grams of each sample were centrifuged at 10, 000 rpm (17105×g) for 10 min. Post-centrifugation, the fluid on the gel surface was drained, and the surface was blotted dry. The samples were then weighed, and WHC was calculated using Equation (2):

$$WHC(\%) = \frac{B}{A} * 100\% \quad (2)$$

Where B is the weight of the emulsion gel (g) after centrifugation, and A is the initial weight of the emulsion gel.

2.5. Cooking performance via oven baking

The procedure described by Wen et al. (2021) was adapted with modifications. Emulsion gel samples were cut into slabs measuring 1.5 cm × 1.5 cm × 1 cm and placed on a preheated aluminium baking tray. The tray and oven were placed at the centre of the oven and preheated to 180 °C for 30 min prior to testing. The samples were then baked at 180 °C, and their appearance was documented every 5 min over a 30-min period using a Nikon D5600 camera (Tokyo, Japan) positioned outside the oven. For comparative analysis, raw pork fat (PF) and beef fat (BF) samples of identical dimensions were subjected to the same baking conditions to assess similarities in fat rendering and cooking behaviour between animal fats and emulsion gels. ImageJ® software

(US National Institutes of Health, Bethesda, USA) was utilized to quantify changes in the surface area of the samples facing the camera throughout the baking process. Following image capture, each frame was imported into ImageJ, converted to 8-bit, and auto-thresholded; the sample silhouette was extracted and its surface area determined with built-in function. The corresponding outline was stored and pseudo-coloured, and super-imposed with successive outlines to generate the multi-coloured contour illustration shown in the figure.

2.6. Synchrotron-FTIR microspectroscopy

The synchrotron-FTIR experiment was performed on Infrared Microspectroscopy (IRM) beamline (Australian Synchrotron, part of ANSTO, Victoria, Australia), using a Bruker Vertex 80v spectrometer coupled with a Hyperion 3000 FTIR microscope and a liquid nitrogen-cooled narrow-band mercury cadmium telluride (MCT) detector (Bruker Optik GmbH, Ettlingen, Germany). The synchrotron-FTIR spectra were obtained within a spectral range of 3800-700 cm^{-1} using 4 cm^{-1} spectral resolution. The experimental setup, acquisition parameters, and data processing methods were described in detail in our previous work (Kim et al., 2023). Three characteristic bands, corresponding to ν(C=O) of esters from lipid triglycerides (1740 cm^{-1}), amide I (1670 cm^{-1}), and polysaccharides (1100-1058 cm^{-1}), were integrated to create chemical images that revealed the distribution of lipids, proteins, and polysaccharides specific for KGM and curdlan gum, based on the laboratory-based FTIR-spectra of the raw ingredients (Fig. S4). ImageJ® software (US National Institutes of Health, Bethesda, USA) was used to create combined maps of lipid-rich, protein-rich, and polysaccharide-rich areas.

2.7. Rheological measurement

All rheological measurements were conducted using a strain-controlled rheometer (TA ARES G2, TA Instruments, New Castle, USA), with temperature monitored and controlled by the Advanced Peltier System (APS), following our previous methods with minor modifications (Wang et al., 2023). The pre-gelled emulsions were loaded onto the lower geometry and gelled in situ. Cross-hatched steel plate geometries (40 mm diameter, upper and lower) were employed to eliminate wall slip. To minimize evaporation, a thin layer of silicon oil was applied to the sample surface, and the geometry was enclosed with a solvent trap cap. Data were collected and analysed using TA TRIOS software version 5.1.1.

2.7.1. Frequency sweep

Small amplitude oscillation shear (SAOS) frequency sweep tests were performed on the prepared emulsions at 25 °C immediately after preparation. The tests were conducted over a frequency range of 0.1–1000 rad/s to evaluate the viscoelastic properties of the emulsion gels. The storage modulus (G') and loss modulus (G'') were recorded. All tests were conducted within the linear viscoelastic region (data not shown).

2.7.2. Gelling behaviours

A single heating pattern was employed to evaluate the gelling behaviour of pre-gelled emulsions. The emulsions were first equilibrated at 25 °C for 2 min, followed by heating from 25 °C to 50 °C at a rate of 5 °C/min. The temperature was held at 50 °C for 15 min, then increased to 85 °C at the same rate and held for 30 min. Finally, the emulsions were cooled back to 25 °C at a cooling rate of 5 °C/min.

2.7.3. Gel strength under large amplitude oscillation

Rheological measurements under large amplitude oscillatory shear (LAOS) were conducted to assess the gel strength of the emulsions. The oscillation strain was varied from 0.01 % to 1000 % with 10 data points per decade, at a frequency of 1 Hz. The 2nd, 3rd, 5th, 7th, and 9th harmonics, including higher harmonic intensity and elastic and viscous Chebyshev decompositions (Ewoldt et al., 2008), were calculated using TA TRIOS software with the Fourier Transform (FT) Rheology Analysis package. Elastic and viscous Lissajous curves were plotted using the MITlaos program (Version 2.2 beta, freeware distributed from MIT-laos@mit.edu).

2.8. Texture profile analysis (TPA)

The texture profile of the emulsion gels and animal fat samples was evaluated using a texture analyzer (Stable Micro Systems TA.XTplusC, Surrey, UK). Samples, including emulsion gels and cooked animal fat at room temperature, were cut into 1.5 cm × 1.5 cm × 1.5 cm slabs for testing. A P50 uniaxial probe was employed to compress the samples. Each sample was compressed twice to 6 mm (40 % of the original height), with a 5-s interval between compressions. Key parameters such as hardness, cohesiveness, springiness, and chewiness were automatically calculated. Each formulation underwent three independent TPA measurements.

2.9. Statistical analyses

All the measurements in this study were done in triplicate. The results are reported as average ± standard deviation. ANOVA results were labelled as superscript of the data using SPSS (version 26.0, IBM Corp., Armonk, NY) with significant difference ($p \leq 0.05$) determined by Duncan's test.

3. Results and discussion

3.1. Macrostructure and morphology

Fig. 1 showcases the visual appearance of emulsion gels formulated with varying concentrations of polysaccharides (PS), including konjac glucomannan (KGM), and different types of fats, beef fat (BF) and pork fat (PF), under both raw (R) and cooked (C) conditions. The emulsion gels exhibited a range of textures and structural integrity, with visible differences in their firmness and cohesiveness. These variations were influenced by the specific composition, especially when the total polysaccharide concentration was altered. Formulations with lower polysaccharide concentrations, such as PS-4 %, resulted in a visibly softer structure that struggled to maintain its overall shape, appearing more like a semi-solid, whereas the others displayed a firmer consistency. This indicates that the gelling network was mainly formed by polysaccharide, since native pea protein usually will not form gel at low concentrations like in the current study (Klost & Drusch, 2019). When there was no pea protein isolate (PPI, 0 %), the gel looked more translucent.

Fig. 2 and Table S1 present the colourimetric measurements of PPI-CUD/KGM emulsion gels and animal fat. The results aligned with the visual appearances observed in Fig. 1. For most samples (excluding PPI-0 %), the colour analysis revealed a light yellowish hue. Increasing the oil and PS content contributed to enhanced lightness (L^* increased from 79.85 ± 1.85 to 86.33 ± 0.67 when oil increased, from 81.83 to 84.08 when PS increased, as detailed in Table S1), with minimal changes observed in the red-green (a^*) and blue-yellow (b^*) axes. Notably, when compared to the reference animal fats, all emulsion gels, except for Oil-40 % and PS-7 %, achieved a similar lightness (L^*) to that of cooked pork fat (Fig. 2A–C). A comparable level of yellowness was measured for all emulsion gel samples, except for 0 %-PPI, when compared to raw beef fat. However, the emulsion gels, excluding 0 %-PPI, showed poor resemblance in the red-green colour axis to any of the animal fat references. On the other hand, the 0 %-PPI sample closely matched the cooked pork fat in all three colour parameters (L^*, a^*, and b^*).

The colour of an emulsion is influenced by the scattering and absorption of light, which depends on factors such as droplet size, droplet concentration, and the chromophores present in the materials used (Wannasin & McClements, 2023). At higher droplet concentrations,

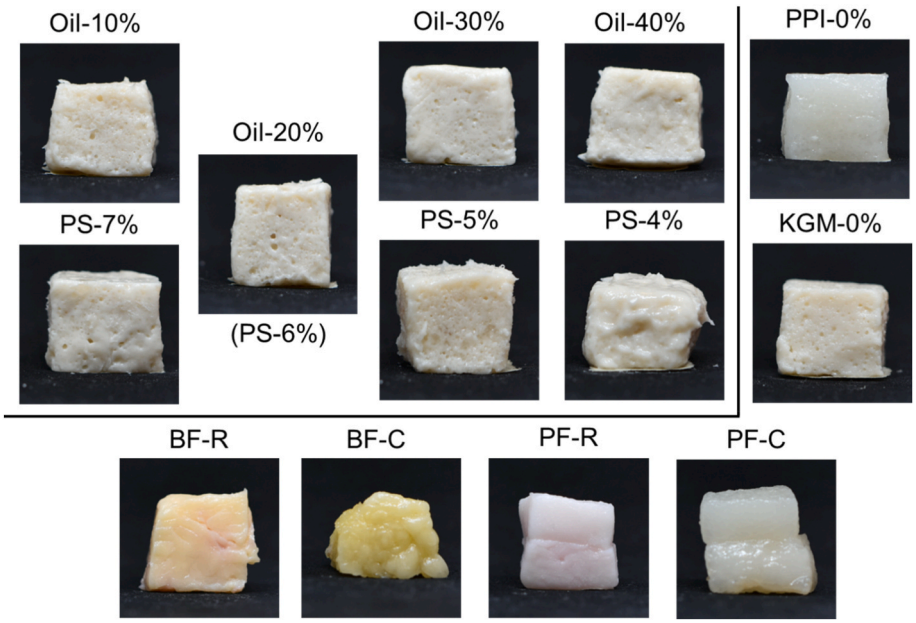

Fig. 1. Emulsion gel appearance with different formulation (PS, polysaccharide concentration; KGM, konjac glucomannan; PPI, pea protein isolate; BF, beef fat; PF, pork fat; R, raw; C, cooked).

lightness increased due to more intense multiple scattering within the emulsion, as observed with increasing oil content (Fig. 2A). There is an inverse relationship between droplet size and lightness, consistent with the findings in Fig. 3D, where lower lightness was observed in samples with larger droplet sizes, such as PS-4 % and KGM-0 %. Regarding the chromatic properties of the emulsion gels, PS and oil content had an insignificant impact on the a^* and b^* values (Fig. 2D–F, 2G-I), likely because PPI is the dominant chromatic component in the gel. Significant differences in a^* and b^* values were only observed in the 0 %-PPI samples. Additionally, the yellowness observed in beef fat is related to the β-carotene content within the fat, which is influenced by the animal's diet (Öztürk-Kerimoglu et al., 2021).

3.2. Cooking and freezing performance

Morphological changes of the emulsion gels during cooking via oven baking were evaluated and compared with animal fats (Fig. 3). Fig. 3A presents time series images showing that higher oil concentrations (30 % and 40 %) lead to more pronounced shrinkage and deformation as cooking progresses. The contour illustrations on the right clearly depict this increased instability in the gel structure with higher oil content. Although this shrinkage was more profound in the emulsion gels, it might actually better mimic the slow release of oil from fat tissues during cooking, which was an expected characteristic of animal fat tissues (Moghtadaei et al., 2021).

In Fig. 3B and C, the effects of varying PS and KGM content on the cooking profiles are shown. Lower PS concentrations (PS-4 %) resulted in significant shrinkage, indicating less structural stability during cooking, similar to the trend observed with higher oil content. In contrast, higher PS and KGM contents provided better shape retention. Fig. 3D compares the cooking profiles of emulsion gels with animal fats (BF and PF). It is evident that pork fat (PF) maintains its structure with limited shrinkage during cooking, while beef fat (BF) shows more pronounced shrinkage.

Fig. 4 presents the normalized changes in surface area for various PPI-CUD/KGM emulsion gel formulations and animal fats over 30 min of oven baking. The samples with 30 % and 40 % oil showed a shrinkage pattern very similar to that of pork fat, indicating that these formulations might mimic the morphological changes of animal fat during cooking. Fig. 4B indicates that gels with higher PS content (PS-7 % and PS-6 %) maintained their surface area more effectively than those with lower PS content, which aligns with the observations from Fig. 3 regarding shape retention. Fig. 4C and D further compare specific formulations, showing that the PPI-0 % and KGM-0 % samples demonstrated more surface area reduction than the corresponding PS-6 % formulations, indicating that both PPI and KGM contributed to structural stability during cooking, which aligned with previous studies to stabilize emulsions using both protein and polysaccharides (Domínguez et al., 2021).

Not only is the cooking stability crucial, but since many plant-based meat alternatives are frozen for storage (Lin et al., 2020), the emulsion gels must also maintain their integrity through the freeze-thaw cycles. Fig. 5 shows the freeze-thaw stability of various PPI-CUD/KGM emulsion gel formulations over five cycles. Fig. 5A reveals that while most oil concentrations maintained an acceptable level of stability, the sample with 40 % oil content showed significant weight loss. This weight loss could be attributed to both water and oil loss, based on our observations, which is consistent with previous studies (Choi et al., 2023). Fig. 5B shows that higher PS content (PS-7 %) improves freeze-thaw stability, minimizing weight loss across cycles. Both PPI and KGM contributed significantly to maintaining weight and thus the structural integrity of the gels during freeze-thaw processes, as shown in Fig. 5C and D, with KGM's effective water-holding capacity playing a key role (Fan et al., 2025).

Using the two most common red meat sources, the current study may be used as a template for specific designs for other fat analogues in different plant-based products, as animal fat types could vary significantly during cooking and storage (Wijarnprecha et al., 2022).

3.3. Microstructure

Fig. 6 presents CLSM images showing the effects of oil and polysaccharide concentration. Fig. 6A illustrates that there was a noticeable increase in droplet size as oil concentration increases from 10 % to 40 %, particularly evidented at 40X magnification. This increase in droplet size might explain the greater and faster shrinkage observed in the 40 % oil sample during cooking (Fig. 3A). Fig. 6B shows the effect of varying PS concentrations, where lower PS content (PS-4 %) resulted in larger and

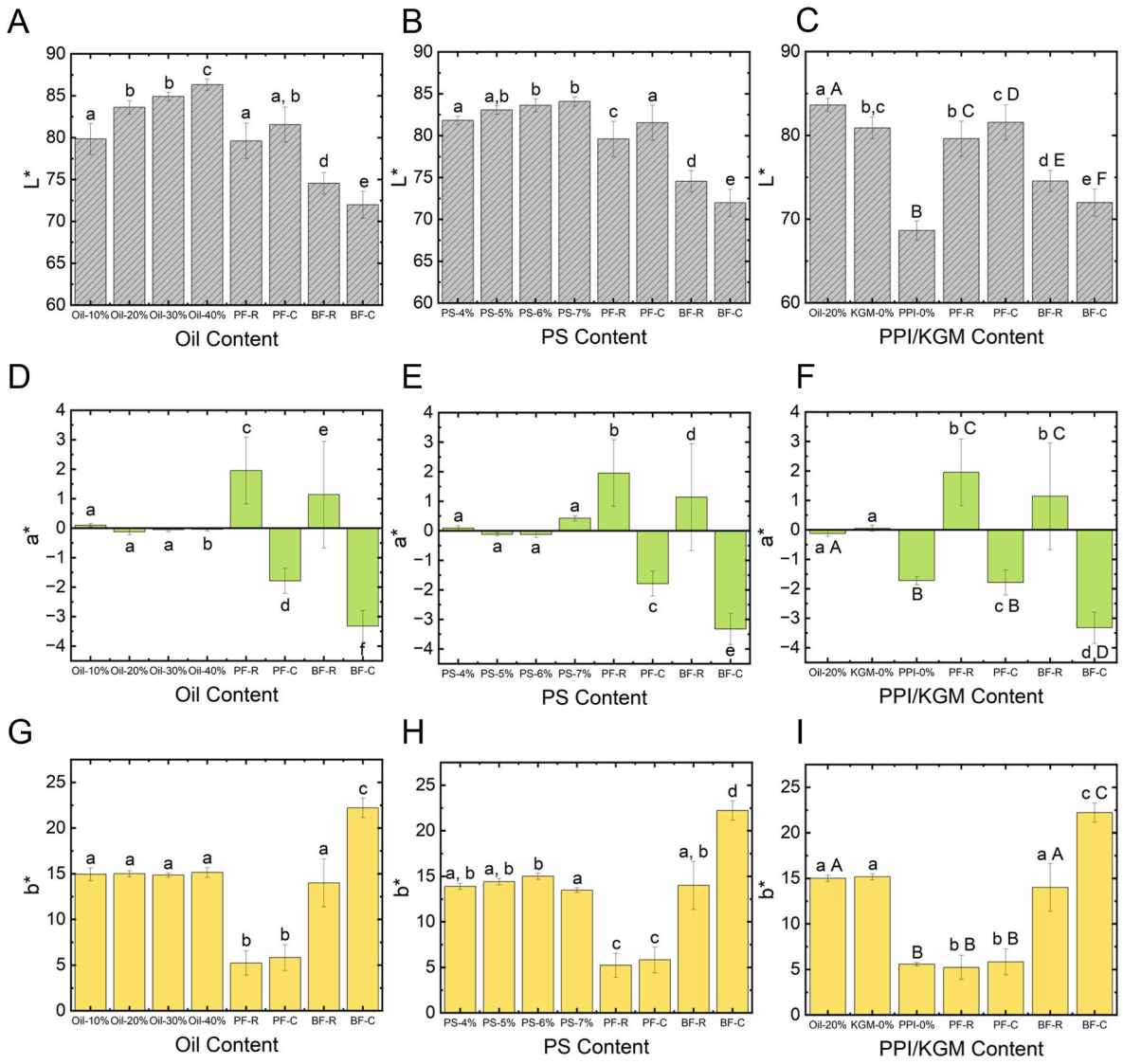

Fig. 2. Colourimetric measurements of PPI-CUD/KGM emulsion gels of various formulations and animal fat (raw and cooked). A-C. Lightness (L^*) values of emulsion gels compared to animal fat. D-F. Red-green axis (a^*) values of emulsion gels compared to animal fat. G-I. Blue-yellow axis (b^*) values of emulsion gels compared to animal fat.

less uniformly distributed droplets, indicating that higher polysaccharide content helps to stabilize the droplet size and distribution within the gel. Because an adequate amount of polysaccharide helps to form the texture of the emulsion gel, creating physical separation that keeps the oil droplets stable within the gel structure (Shao et al., 2020).

Fig. 6C compares the microstructures of gels without KGM or PPI. The absence of KGM resulted in a structure with larger and irregular droplets, while the absence of PPI lead to even larger droplets and a less uniform distribution. This confirmed that PPI is essential for proper encapsulation of the oil as the emulsifier in this emulsion gel. The role of protein as the emulsifier in stabilizing oil droplets within emulsion gels has been widely reported, particularly in systems using solid fats to mimic animal fat (Dreher et al., 2020). However, our study focuses on oil-in-water emulsions without solid fats, examining how varying oil and polysaccharide concentrations affected droplet stability. Fig. 6D quantified these observations, showing the average oil droplet size in various formulations (droplet size distribution can be found in Fig. S1). Most gels showed average oil droplets size around or below 10 μm. It confirmed that formulations with higher oil content and lower PS content tended to have larger droplets, while those with both polysaccharides and PPI showed smaller and more stable droplets.

Based on the observations, we propose gelling mechanism of the emulsion gels in Fig. 7, highlighting the unique role of each ingredient in the system. In optimal conditions, the oil droplets should be uniformly distributed within the gel structure, with droplets of similar size (Fig. 7A). The stabilization of emulsion gels is primarily achieved through a combination of steric stabilization provided by the polysaccharides (Shi et al., 2023) and protein adsorption at the oil-water interface, which reduces surface tension and prevents coalescence of the oil droplets (Li et al., 2020). Fig. 7B further shows that with a 40 % oil concentration, large droplets are formed, prone to breakdown. This is evident in Fig. 6A where we observed that increasing oil concentration to 40 % led to larger, less stable droplets, correlating with the more significant shrinkage seen in Fig. 3A during cooking. In Fig. 7C, the crucial role of PPI in this stabilization process is illustrated; without PPI, the oil droplets are not effectively encapsulated, resulting in large, unstable droplets (as shown in Fig. 6C). KGM helped to stabilize the emulsion before gelling by hydrogen-bond and electrostatic interactions, where KGM chains at the interface to provide steric-hydration repulsion against droplet coalescence (Jian et al., 2015; Z. Liu et al., 2021). Lastly, Fig. 7D shows that KGM helps maintain smaller oil droplet sizes; in its absence, the oil droplets become unstable,

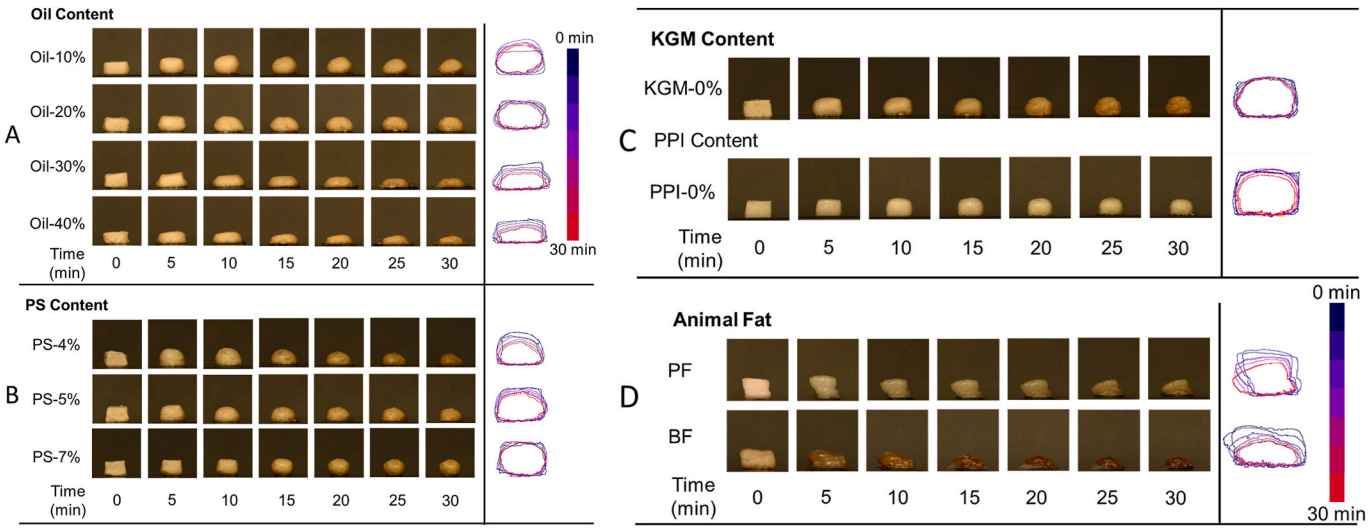

Fig. 3. Cooking profile of PPI-CUD/KGM emulsion gels of various formulations under oven cooking conditions. A. Time series images of samples at varying oil content. B. Time series images of samples at varying PS content. C. Time series images of KGM-0 % and PPI-0 %. The profile of the sample at each time point was taken and overlayed to construct a contour illustration. The illustration is appended to the right side of each formulation. (PS, polysaccharide concentration; KGM, konjac glucomannan; BF, beef fat; PF, pork fat; R, raw; C, cooked).

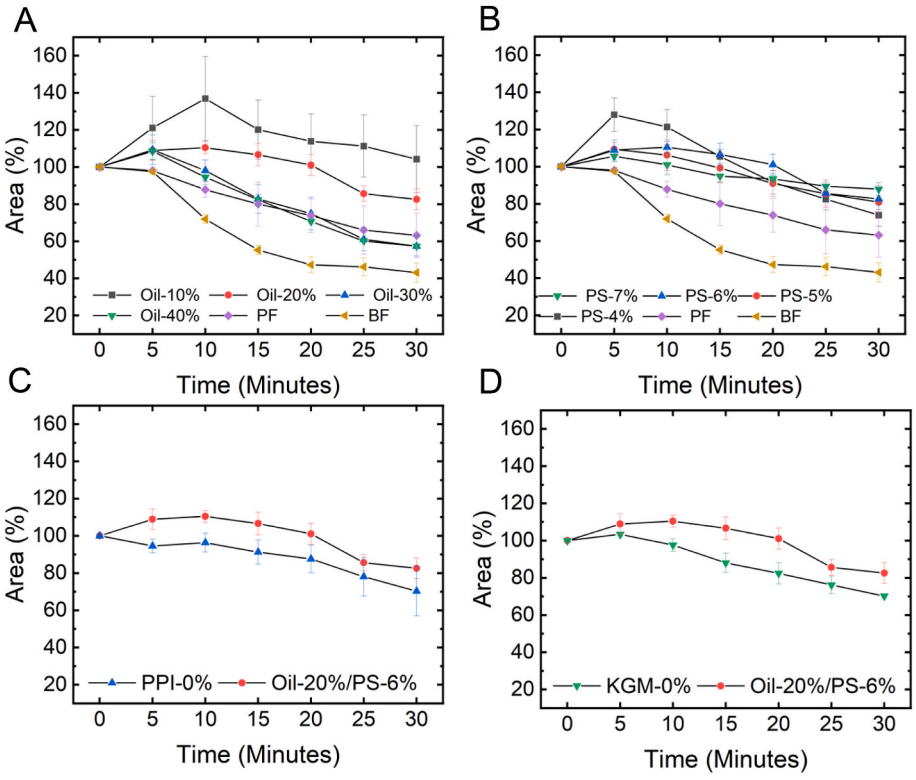

Fig. 4. Normalized changes in surface area of various PPI-CUD/KGM emulsion gel formulations and animal fat over 30 min of oven cooking. A. Samples at varying oil content. B. Samples at varying PS content C. Comparison of PPI-0 % and Oil-20 %/PS-6 %. D. Comparison of KGM-0 % and Oil-20 %/PS-6 %. (PS, polysaccharide concentration; KGM, konjac glucomannan; PPI, pea protein isolate; BF, beef fat; PF, pork fat).

which aligns with the observations from Fig. 6C. Upon heating, KGM undergoes a coil-helix transition, forming an elastic network that increases continuous-phase viscosity and physically traps the emulsified droplets, thereby restricting oil migration during cooking (W. Lu et al., 2018). The sample without curdlan also will not form stable emulsion gel (diagram showed in Fig. S2).

To further validate the hypothesis in Fig. 7, we employed synchrotron-FTIR microspectroscopy to examine the co-localization of lipids, carbohydrates, and proteins within the emulsion gel network at varying oil concentrations (10 %–40 %). The synchrotron-FTIR technique allows for direct chemical imaging that reveals the distributions of proteins, polysaccharides, and oils in analysed samples with a spatial resolution of 2–3 μm (Kim et al., 2023). Representative average spectra extracted from lipid-rich, protein-rich, and carbohydrate-rich regions are shown in Fig. S3. The lipid distribution in Fig. 8A with concentration indicated by the absorption intensity following the colour bar, correlates

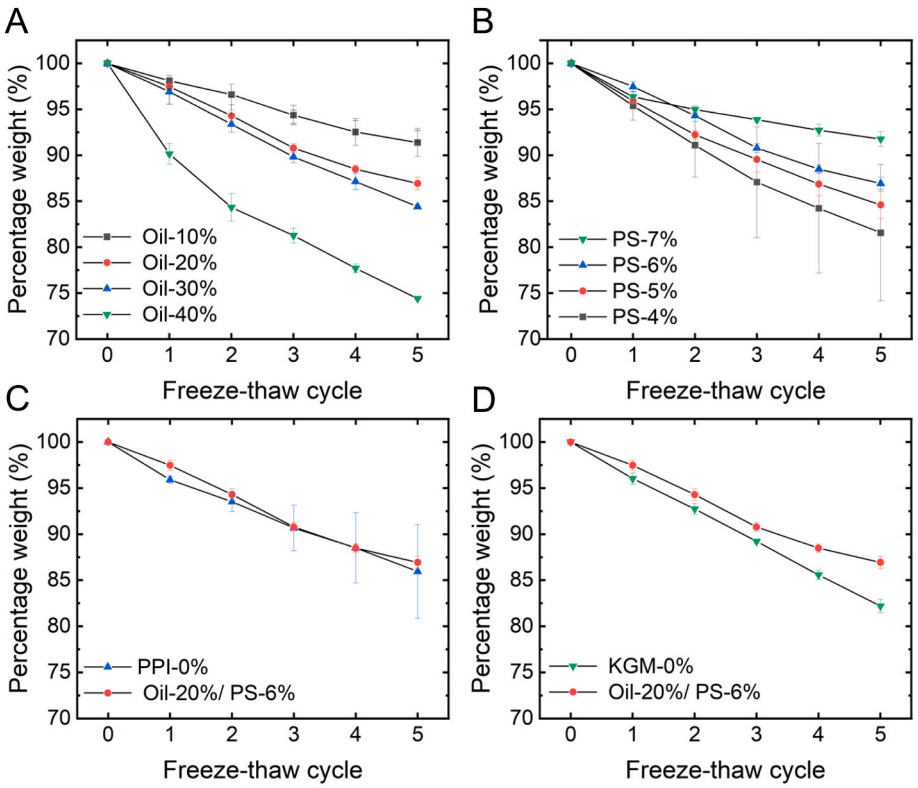

Fig. 5. Freeze-thaw stability of emulsion gels of various formulations over five cycles. A: Percentage weight of samples at varying oil content. B. Percentage weight of samples at varying polysaccharide content. C. Freeze-thaw stability of PPI-0 % compared to Oil-20 %/PS-6 %. D. Freeze-thaw stability of KGM-0 % compared to Oil-20 %/PS-6 %. (PS, polysaccharide concentration; KGM, konjac glucomannan; PPI, pea protein isolate).

well with the gel composition and increases as oil concentration rises, particularly at 40 × magnification (Fig. 6A). The distribution of carbohydrates (including curdlan and KGM) in Fig. 8B, on the other hand, remained relatively stable in all three oil concentrations. This indicated that carbohydrates were the key component that form the primary structural framework supporting the emulsion gel, consistent with previous studies that used curdlan (B. Cui et al., 2022) and KGM (Jeong et al., 2023). The protein distribution primarily surrounded the lipids (Fig. 8C).

To better understand the co-localization of these components, we employed an alternative visualization approach to present multiple components using distinct colours to represent lipids (L, red), proteins (P, blue), and carbohydrates (C, green) within the emulsion gel network at varying oil concentrations (10 %–40 %), as shown in Fig. 8D–G. The key observation was that proteins (blue) closely attached to the lipid droplets (red areas), indicating a strong protein-lipid interaction within the gel due to the amphiphilic interfacial properties of the proteins (Dong et al., 2024), as depicted in Fig. 8D. As oil concentration increased, proteins continued to co-localize with lipid droplets (Fig. 8G), while carbohydrates helped maintain the structural integrity of the gel by forming thermally irreversible networks from curdlan (Wang et al., 2023). However, it should be noted that their distribution becomes less uniform at higher oil contents. These findings are consistent with the trends observed in the CLSM images and further support our hypothesis presented in Fig. 7.

3.4. Rheological behaviours and texture analysis

3.4.1. Emulsion before gelation

Fig. 9 illustrates the frequency sweep results for emulsion gels with varying oil and polysaccharide concentrations. The storage modulus (G') and loss modulus (G'') increased with higher oil concentrations, as seen in Fig. 9A and B. Specifically, samples with higher oil content exhibited greater modulus values, with the storage modulus being slightly higher than the loss modulus. The highlighted yellow box in Fig. 9A shows that the difference in storage modulus is more pronounced at lower angular frequencies, becoming less distinct at higher frequencies. The impact of polysaccharide content was notably more significant (Fig. 9C and D), with the modulus values increasing dramatically, by up to three orders of magnitude, as polysaccharide concentration rises from 4 % to 7 %. This suggested that an appropriate level of polysaccharides is crucial for maintaining the stability of the emulsion before gelation occurs, as they increased the viscosity of the aqueous phase and help keep the oil droplets separated until the next processing step (Dickinson, 2019). This observation is consistent with the confocal microscopic images in Fig. 6B, where it was evident that at polysaccharide concentrations of 4 % or 5 %, the emulsion showed larger oil droplets and became less stable.

3.4.2. Gelling process

Fig. 10 demonstrates how heating, isothermal holding, and cooling processes can be used to manipulate the structure formation of the emulsion gel, which is crucial for its overall stability. During heating (Fig. 10A), the sample underwent two isothermal stages, one at 50 °C and another at 85 °C. At 50 °C, the curdlan in the sample formed a weak, reversible gel structure (Wang et al., 2023), which was reflected in a slight increase in storage modulus, as demonstrated in Fig. 10D. This early-stage gelation is important as it quickly stabilizes the oil droplets within the network, forming a more robust structure to undergo the following heating process (H. Li, Meng, et al., 2022).

As temperature reaches 85 °C, the modulus values showed minimal changes during the heating process. However, during the 85 °C isothermal holding stage, the modulus showed a significant change, especially in the sample with 10 % oil content, as depicted in Fig. 10E. During this 30-min isothermal period, the emulsion gel formed a denser and more stable structure due to the irreversible gelation of curdlan at

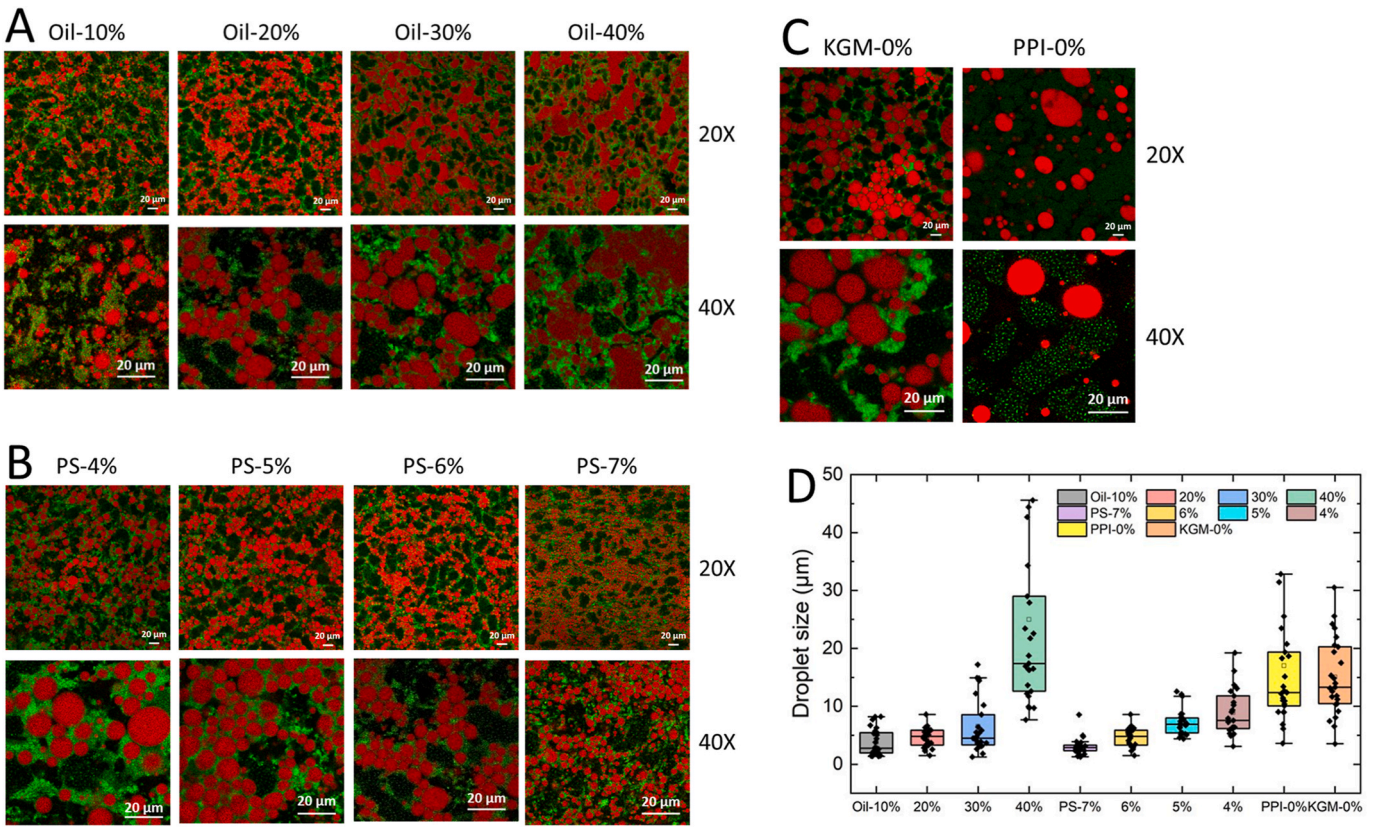

Fig. 6. Confocal laser scanning microscopy of emulsion gels as affected by oil concentration (A) and different polysaccharide concentration (B); emulsion gels without KGM or PPI (C); average oil droplet size in emulsion gels with different formulation (D). All scale bars in picture represent 20 μm. (PS, polysaccharide concentration; KGM, konjac glucomannan; PPI, pea protein isolate).

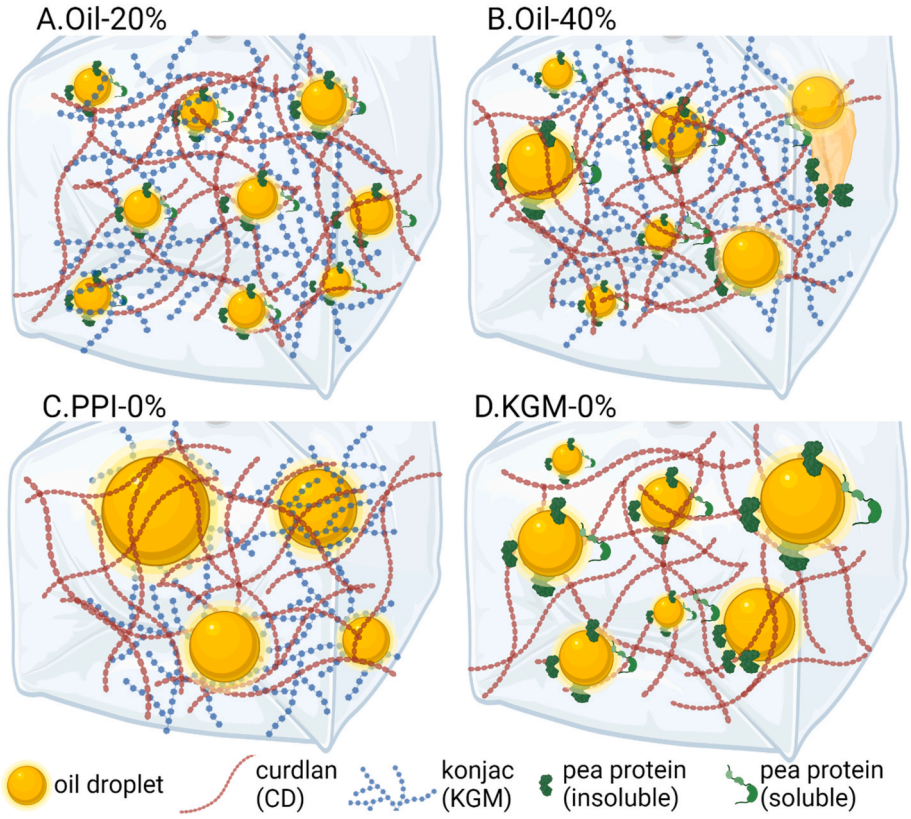

Fig. 7. Diagram of proposed gelling mechanism of the emulsion gels. Created using Biorender (with permission for publication).

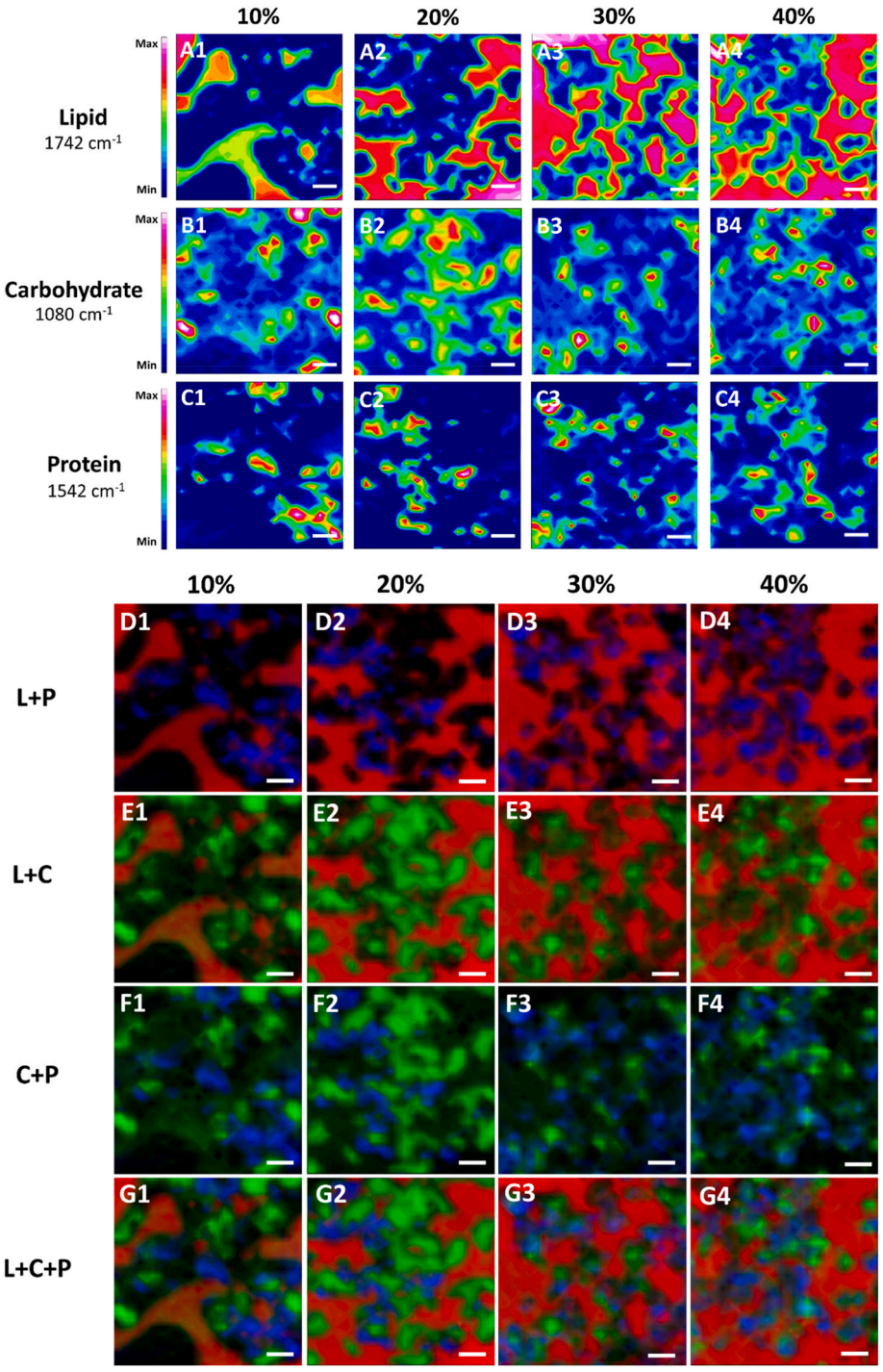

Fig. 8. (A–C)Synchrotron-FTIR chemical images showing distributions of lipid, carbohydrate, and protein within the emulsion gel network at varying oil concentrations (10 %–40 %). (D–G) RGB composite images revealing the co-localization of lipids (L, red), proteins (P, blue), and carbohydrates (C, green) in different combinations. Scale bars in the picture represent 20 μm.

this temperature (Aquinas et al., 2022; S.-Y. Liu et al., 2023).

During the cooling stage following the 85 °C isothermal period, all samples exhibited a significant increase in modulus, which was consistent with previous observations of emulsion gel systems (Lorenzo et al., 2018). After cooling, the emulsion gels maintained stability, with final modulus values inversely related to oil content, as lower oil content allows more polysaccharides to form cross-links within the aqueous phase especially for curdlan gum (C. Zhang et al., 2023), leading to a denser structure (also shown in Fig. 6).

Although its individual contribution to modulus cannot be quantified separately, KGM is essential for maintaining the stability of the emulsion system during the initial stages. Curdlan alone, with its lower viscosity, requires KGM to stabilize the system effectively (Wei et al., 2021). The gel will have much lower modulus value without KGM, both before gelation and the final stage after gelation, as shown in Fig. S6.

3.4.3. *Texture profile analysis (TPA)*

The TPA results for PPI-CUD/KGM emulsion gels of various formulations are presented in Fig. 11 and Table S2. As shown in Fig. 11A–C, both oil and PS content significantly influenced the hardness and

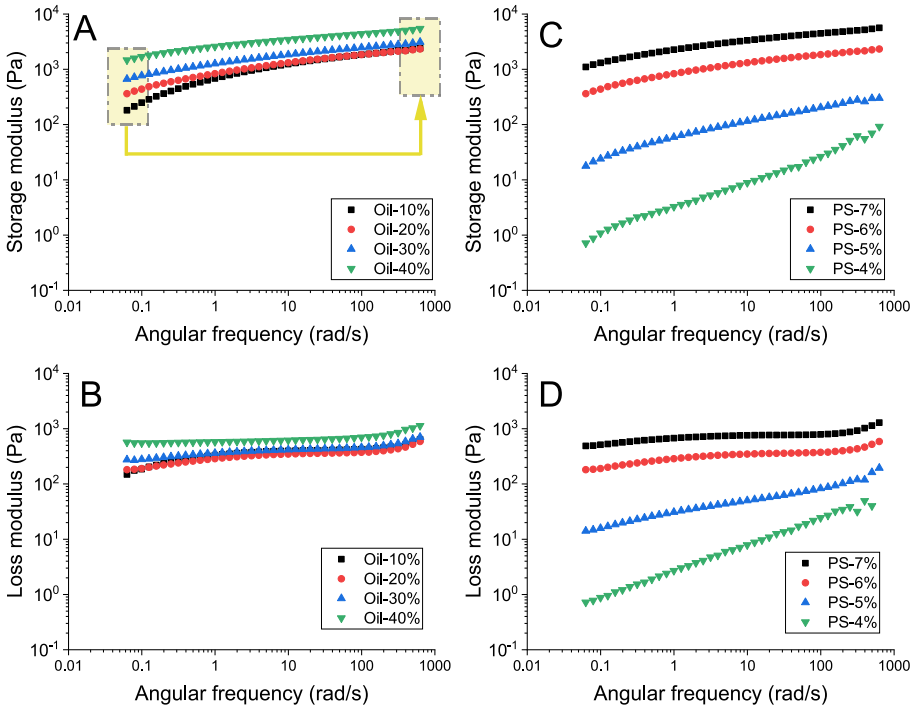

Fig. 9. Frequency sweep with SAOS range on emulsion gels with different oil concentrations (A: storage modulus; B: loss modulus), or different polysaccharide concentration (PS) (C: storage modulus; D: loss modulus).

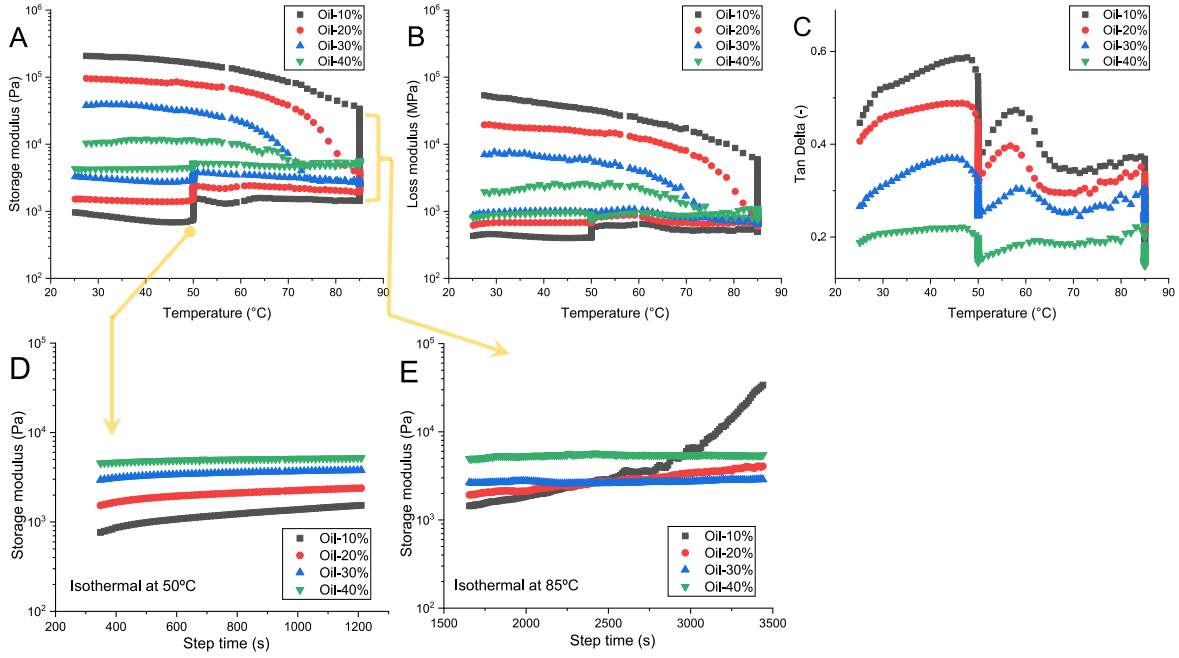

Fig. 10. Effects of heating temperatures on the gelling behaviour of emulsion gels with different oil concentration upon heating (up to 85 °C), cooling (to 25 °C) and isothermal (at 50 °C and 85 °C respectively): A. Storage modulus; B. Loss modulus; C. Tan Delta for heating and isothermal stages; D. Storage modulus at 50 °C isothermal; E. Storage modulus at 85 °C isothermal.

chewiness of the emulsion gels. These properties increased with rising oil and PS content, peaking at the highest levels tested, particularly in the Oil-40 % and PS-7 % samples. Conversely, springiness and cohesiveness, illustrated in Fig. 11D–F, were largely independent of oil content. While increasing PS content had a slight positive effect on springiness, cohesiveness remained unaffected by PS content, showing no significant differences.

The addition of KGM notably increased hardness and chewiness, as demonstrated by the 38.5 % (136.21 ± 5.74 N to 188.71 ± 27.95 N) and 198.7 % (7.90 ± 0.21 N to 23.54 ± 7.69 N) increases, respectively, compared to KGM-0 % samples (Fig. 11C). KGM also enhanced springiness and cohesiveness by 34.5 % and 55.0 %, respectively (Fig. 11F). The observed trends in hardness and chewiness aligned with the rheological data, where higher gel strength corresponds to increased

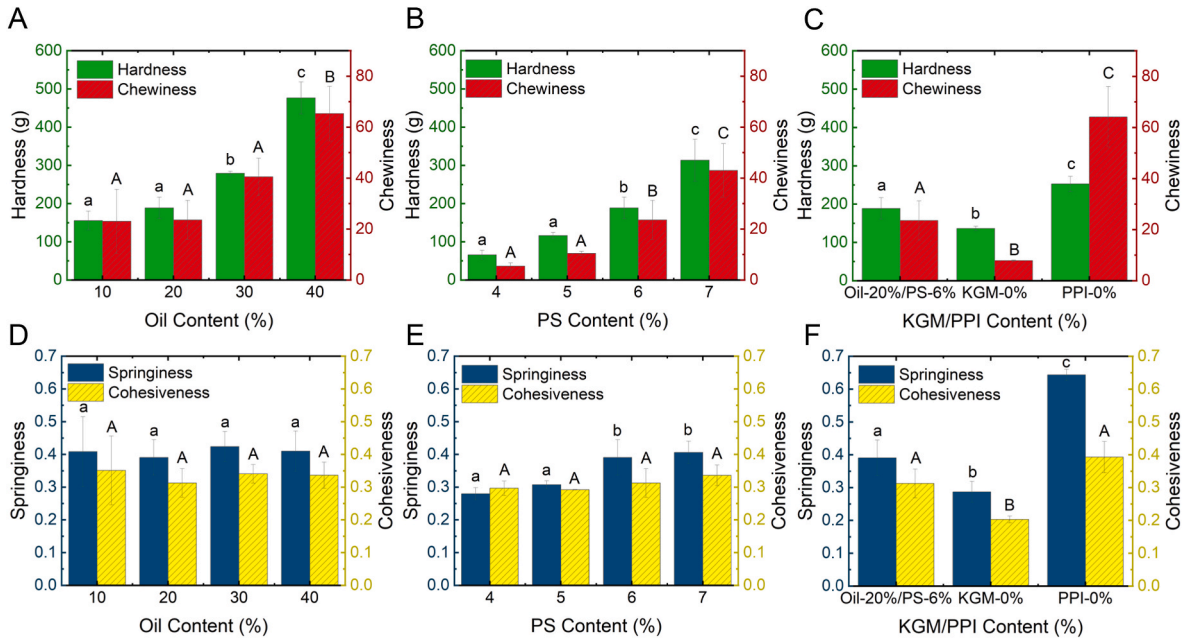

Fig. 11. Texture profile analysis (TPA) of varying PPI-CUD/KGM emulsion gel formulations. A-C. The hardness and chewiness of emulsion gels. D-F. The springiness and cohesiveness of emulsion gels. A and D. Varying oil content. B and E. Varying PS content. C and F. Comparison of Oil-20 %/PS-6 % with KGM-0 % and PPI-0 % samples. The superscript letter indicates significant difference ($p < 0.05$). (PS, polysaccharide concentration; KGM, konjac glucomannan; PPI, pea protein isolate).

hardness and chewiness. The trends in TPA values for hardness, chewiness, springiness, and cohesiveness in PPI-0 % samples compared to Oil-20 %/PS-6 % samples differed from the lower gel strength observed in rheological tests. This is because the two methods serve different purposes: rheology, particularly small amplitude oscillation, tracks the structure formation under minimal deformation, whereas TPA focuses on structure breakdown during processes like cooking or chewing, which involve large deformations. Such difference in the trends from SAOS rheology and TPA has also been reported in emulsion gel for baking application (Youdong Li, Duan, et al., 2024) and hydrogels prepared from egg white protein (Dai et al., 2021), where, like current study, both techniques provide complementary insights into the gel's behaviour throughout its lifecycle. Additionally, the oiling-off observed post-gelation and higher initial water content may have enhanced the rehydration and gelation of the polysaccharides.

Compared to animal fats, the emulsion gels produced in this study exhibited a significantly softer and less chewy texture than beef and pork fat at room temperature. Specifically, the hardest emulsion gel sample (Oil-40 %) reached only 18.2 % of the hardness of pork fat (PF) and 14.3 % of beef fat (BF), as shown in Table S2. However, the emulsion gels more closely resembled cooked pork fat in terms of cohesiveness and springiness. The substantial textural differences may be attributed to the presence of fat with high solid fat content (SFC) and the stronger mechanical properties of collagen, as reported in previous studies (Dreher et al., 2020; Wijarnprecha et al., 2022). It is also worth noting that the hardness level of our gels are 10–100 times higher than a recent study using curdlan gum alone to mimic animal fat (3.02–6.64 N as reported by Choi et al. (2024)), highlighting the significant role of developing double polysaccharide networks using both curdlan and KGM to more closely mimic specific animal fat.

3.4.4. *Large amplitude oscillation shear (LAOS)*

Building on the previous rheological data presented in Fig. 10 and the TPA results in Fig. 11, where we observed differences in the modulus

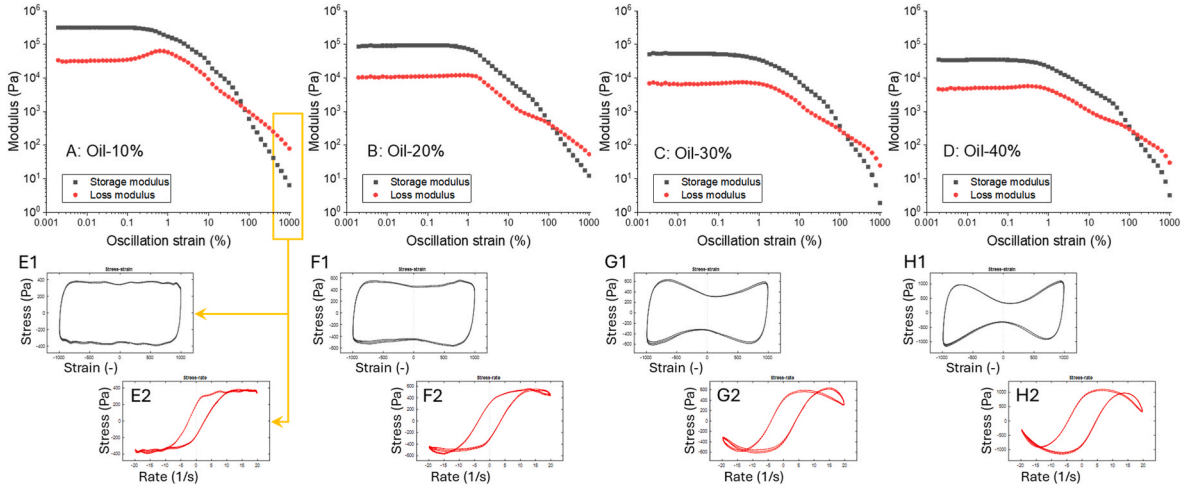

Fig. 12. Strain sweep curves of curdlan/KGM/pea protein emulsion gels in LAOS regime at different oil concentration (A/B/C/D: 10/20/30/40 %); (E1) – (H1) elastic Lissajous curve, (E1) – (H1) elastic Lissajous curve, at oil concentration of 10 %–40 %.

trends at small strains compared to the hardness measurements, we sought to further investigate the gel structure under larger strain conditions. Fig. 12 presents the strain sweep curves of curdlan/KGM/pea protein emulsion gels in the LAOS regime at different oil concentrations (10 %, 20 %, 30 %, 40 %). All samples exhibited a characteristic decrease in both modulus with increasing strain, indicating the transition from the linear viscoelastic region (LVR) to non-linear behavior (Wang & Selomulya, 2022). The samples with higher oil concentrations (Fig. 12C and D) exhibited a more pronounced decrease in storage modulus compared to those with lower oil content (Fig. 12A and B), suggesting that higher oil content lead to a less stable gel structure under large deformation (Joyner, 2021).

Additionally, the elastic Lissajous curves (Fig. 12E1-H1) and viscous Lissajous curves (Fig. 12E2-H2) provide further insights into the non-linear behaviour of the gels at different oil concentrations. The shapes of these curves indicate the material's response to strain and shear rate, where more elliptical curves reflect greater non-linearity and energy dissipation (Hyun et al., 2011). As the oil concentration increased, the Lissajous curves became more elliptical, particularly in the 30 % and 40 % oil samples, indicating that these gels underwent greater structural deformation and energy loss under large strain conditions (Duvarci et al., 2017). These characteristics are important for achieving a texture

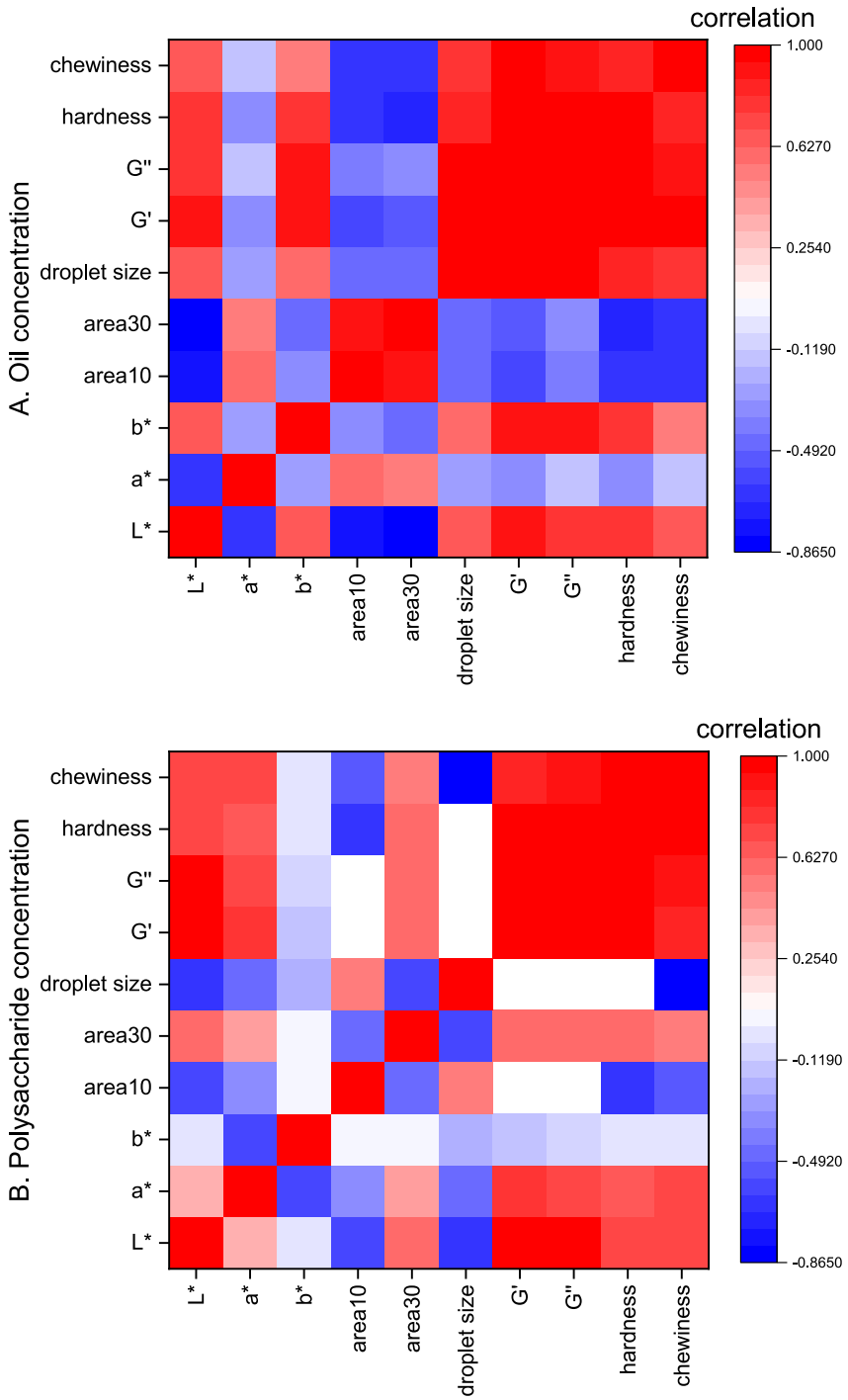

Fig. 13. Correlations between the colour (L^*, a^*, b^*), cooking shape change (area10/30 represent the shape of emulsion gels after 10/30 min cooking), oil droplet size, texture (G', G'', hardness, chewiness). (A) correlations at different oil concentrations; (B) correlations at different polysaccharide concentrations.

that closely mimics animal fat in food applications, though further analysis of specific parameters such as strain stiffening and shear thinning after cooking could provide deeper insights (Donley et al., 2020).

Fig. 13 illustrates the correlation between various properties of the emulsion gels, including colour (L^*, a^*, b^*), cooking-induced shape changes (area after 10 and 30 min), oil droplet size, and textural parameters (G', G'', hardness, chewiness) at different oil concentrations (Fig. 13A) and polysaccharide concentrations (Fig. 13B). The correlations revealed that at higher oil concentrations, there was a stronger positive correlation between oil droplet size and both G'' and hardness, indicating that larger droplets contributed to increased hardness and loss modulus. Meanwhile, L^* (lightness) showed a negative correlation with these textural parameters, suggesting that lighter gels tend to have lower hardness and chewiness. The area (area10/30) showed a strong negative correlation with all structural parameters as anticipated, since stronger structural integrity resulted in less changes during cooking. Notably, animal fats exhibited stronger structural performance, yet retained a soft texture and gradual transformation during cooking, highlighting the need for further research to better mimic the processing profile of animal fat tissues.

4. Conclusions

The unique role of varying oil and polysaccharide concentrations in regulating the texture and structural stability of curdlan/KGM/PPI emulsion gels was presented in this study. Our findings provide a comprehensive analysis of how these compositional factors influence macrostructure, microstructure, and rheological properties of the gels, leading to variations in stability, texture, and performance during cooking and freeze-thaw circles. The macrostructural analysis suggests that higher polysaccharide concentrations, particularly when combined with PPI, may enhance firmness and cohesiveness of the emulsion gels. During cooking and freezing, formulations with increased oil and polysaccharide content appeared to maintain structural integrity more effectively. Microstructural assessments further indicated that oil droplet distribution and encapsulation play a key role in stabilizing the gel matrix, especially in the presence of PPI. Rheological evaluations showed that ingredient composition influences viscoelastic properties, with both storage and loss moduli affected by oil and polysaccharide levels. Although the emulsion gels could not mimic all the changes in properties of animal fat tissues referenced in this study, our findings can be used as a foundation to understand how the composition of oil, polysaccharide, and protein content could be related to various properties of emulsion gels. This strategy could enable the replacement of animal fats with lower saturated fatty acid oils. Further studies are needed to explore the long-term stability, sensory attributes, and potential applications of these emulsion gels in a wider range of food products.

CRediT authorship contribution statement

Yong Wang: Writing – original draft, Visualization, Supervision, Methodology, Investigation, Funding acquisition, Formal analysis, Data curation, Conceptualization. **Canice Chun-Yin Yiu:** Writing – original draft, Visualization, Methodology, Investigation, Formal analysis, Data curation, Conceptualization. **Woojeong Kim:** Writing – original draft, Visualization, Methodology, Formal analysis, Data curation. **Jitraporn Vongsvivut:** Writing – review & editing, Visualization, Data curation. **Weibiao Zhou:** Writing – review & editing, Methodology. **Cordelia Selomulya:** Writing – review & editing, Supervision, Resources, Project administration, Methodology, Funding acquisition, Conceptualization.

Declaration of competing interest

The authors declare that they have no known competing financial interests or personal relationships that could have appeared to influence the work reported in this paper.

Acknowledgement

The synchrotron-FTIR experiment was performed on the Infrared Microspectroscopy (IRM) beamtime at the Australian Synchrotron, part of ANSTO, through the merit-based access (Proposal ID. 21399). The installation of TA ARES G2 rheometer at UNSW Sydney is supported by the UNSW Research Infrastructure Scheme (RIS) grant scheme. The authors acknowledge the support from ARC DP250101468 (Selomulya, Wang, and Zhou).

Appendix A. Supplementary data

Supplementary data to this article can be found online at https://doi.org/10.1016/j.foodhyd.2025.111807.

Data availability

Data will be made available on request.

References

Aquinas, N., Bhat M, R., & Selvaraj, S. (2022). A review presenting production, characterization, and applications of biopolymer curdlan in food and pharmaceutical sectors. *Polymer Bulletin, 79*(9), 6905–6927.

Burger, T. G., & Zhang, Y. (2019). Recent progress in the utilization of pea protein as an emulsifier for food applications. *Trends in Food Science & Technology, 86*, 25–33.

Cheng, Z., Qiu, Y., Bian, M., He, Y., Xu, S., Li, Y., Ahmad, I., Ding, Y., & Lyu, F. (2024). Muscle fibrous structural design of plant-based meat analogs: Advances and challenges in 3D printing technology. *Trends in Food Science & Technology, 147*, Article 104417.

Choi, M., Choi, H. W., Jo, M., Hahn, J., & Choi, Y. J. (2024). High-set curdlan emulsion gel fortified by transglutaminase: A promising animal fat substitute with precisely simulated texture and thermal stability of animal fat. *Food Hydrocolloids, 154*, Article 110063.

Choi, M., Choi, H. W., Kim, H. E., Hahn, J., & Choi, Y. J. (2023). Mimicking animal adipose tissue using a hybrid network-based solid-emulsion gel with soy protein isolate, agar, and alginate. *Food Hydrocolloids, 145*, Article 109043.

Cui, B., Mao, Y. Y., Liang, H. S., Li, Y., Li, J., Ye, S. X., Chen, W. X., & Li, B. (2022). Properties of soybean protein isolate/curdlan based emulsion gel for fat analogue: Comparison with pork backfat. *International Journal of Biological Macromolecules, 206*, 481–488.

Cui, X., Saleh, A. S. M., Yang, S., Wang, N., Wang, P., Zhu, M., & Xiao, Z. (2023). Oleogels as animal fat and shortening replacers: Research advances and application challenges. *Food Reviews International, 39*(8), 5233–5254.

Dai, Y., Zhao, J., Gao, J., Deng, Q., Wan, C., Li, B., & Zhou, B. (2021). Heat- and cold-induced gels of desalted duck egg white/gelatin mixed system: Study on rheological and gel properties. *Food Hydrocolloids, 121*, Article 107003.

de Souza Paglarini, C., de Figueiredo Furtado, G., Honório, A. R., Mokarzel, L., da Silva Vidal, V. A., Ribeiro, A. P. B., Cunha, R. L., & Pollonio, M. A. R. (2019). Functional emulsion gels as pork back fat replacers in Bologna sausage. *Food Structure, 20*, Article 100105.

Dickinson, E. (2019). Strategies to control and inhibit the flocculation of protein-stabilized oil-in-water emulsions. *Food Hydrocolloids, 96*, 209–223.

Dobson, S., & Marangoni, A. G. (2024). Fat stabilization techniques for the reduction of oil loss in high protein plant-based cheese. *Food Hydrocolloids, 156*, Article 110362.

Domínguez, R., Munekata, P. E. S., Pateiro, M., López-Fernández, O., & Lorenzo, J. M. (2021). Immobilization of oils using hydrogels as strategy to replace animal fats and improve the healthiness of meat products. *Current Opinion in Food Science, 37*, 135–144.

Dong, C., Zhao, J., Wang, L., Wang, X., Jiang, J., & Bi, J. (2024). Understanding the textural enhancement of low-salt myofibrillar protein gels filled with pea protein pre-emulsions through interfacial behavior: Effects of structural modification and oil phase polarity. *Food Chemistry, 460*, Article 140632.

Donley, G. J., Singh, P. K., Shetty, A., & Rogers, S. A. (2020). Elucidating the G'' overshoot in soft materials with a yield transition via a time-resolved experimental strain decomposition. *Proceedings of the National Academy of Sciences of the U S A, 117*(36), 21945–21952.

Dreher, J., Blach, C., Terjung, N., Gibis, M., & Weiss, J. (2020). Influence of protein content on plant-based emulsified and crosslinked fat crystal networks to mimic animal fat tissue. *Food Hydrocolloids, 106*.

Duarte, C. M., Bruhn, A., & Krause-Jensen, D. (2022). A seaweed aquaculture imperative to meet global sustainability targets. *Nature Sustainability, 5*(3), 185–193.

Duvarci, O. C., Yazar, G., & Kokini, J. L. (2017). The comparison of LAOS behavior of structured food materials (suspensions, emulsions and elastic networks). *Trends in Food Science & Technology, 60*, 2–11.

Ewoldt, R. H., Hosoi, A. E., & McKinley, G. H. (2008). New measures for characterizing nonlinear viscoelasticity in large amplitude oscillatory shear. *Journal of Rheology, 52*(6), 1427–1458.
Fan, J., Chen, Z., Wang, H., Zeng, Z., Zhou, M., Lu, M., Li, Y., Qin, X., & Liu, X. (2025). Enhancing freeze-thaw stability of frozen dough with deacetylated konjac glucomannan: The role of degree of deacetylation. *Food Hydrocolloids, 158*, Article 110540.
Fontes-Candia, C., Martínez-Sanz, M., Gómez-Cortés, P., Calvo, M. V., Verdú, S., Grau, R., & López-Rubio, A. (2023). Polysaccharide-based emulsion gels as fat replacers in Frankfurter sausages: Physicochemical, nutritional and sensorial evaluation. *Lwt, 180*, Article 114705.
Gómez-Estaca, J., Pintado, T., Jiménez-Colmenero, F., & Cofrades, S. (2020). The effect of household storage and cooking practices on quality attributes of pork burgers formulated with PUFA- and curcumin-loaded oleogels as healthy fat substitutes. *Lwt, 119*, Article 108909.
Guan, X., Fei, Z., Wang, L., Ji, G., Du, G., Ma, Z., & Zhou, J. (2025). Engineered streaky pork by 3D co-printing and co-differentiation of muscle and fat cells. *Food Hydrocolloids, 158*, Article 110578.
Guo, J., Cui, L., & Meng, Z. (2023). Oleogels/emulsion gels as novel saturated fat replacers in meat products: A review. *Food Hydrocolloids, 137*, Article 108313.
Guo, B., Liang, Y., & Dong, R. (2023). Physical dynamic double-network hydrogels as dressings to facilitate tissue repair. *Nature Protocols, 18*(11), 3322–3354.
Heck, R. T., Santos, B. A. D., Lorenzo, J. M., Ruiz-Capillas, C., Cichoski, A. J., de Menezes, C. R., & Campagnol, P. C. B. (2022). Chapter 18 - Replacement of saturated fat by healthy oils to improve nutritional quality of meat products. In J. M. Lorenzo, P. E. S. Munekata, M. Pateiro, F. J. Barba, & R. Domínguez (Eds.), *Food lipids* (pp. 461–487). Academic Press.
Hirashima, M., Takaya, T., & Nishinari, K. (1997). DSC and rheological studies on aqueous dispersions of curdlan. *Thermochimica Acta, 306*(1), 109–114.
Huang, L., Liu, S., Wang, Y., Li, H., Cao, J., & Liu, X. (2023). Effect of cooking methods and polysaccharide addition on the cooking performance of cubic fat substitutes. *Lwt, 181*, Article 114741.
Huang, L., Ren, Y. Q., Li, H., Zhang, Q. B., Wang, Y., Cao, J. N., & Liu, X. Q. (2022). Create fat substitute from soybean protein Isolate/Konjac glucomannan: The impact of the protein and polysaccharide concentrations formulations. *Frontiers in Nutrition, 9*.
Hyun, K., Wilhelm, M., Klein, C. O., Cho, K. S., Nam, J. G., Ahn, K. H., Lee, S. J., Ewoldt, R. H., & McKinley, G. H. (2011). A review of nonlinear oscillatory shear tests: Analysis and application of large amplitude oscillatory shear (LAOS). *Progress in Polymer Science, 36*(12), 1697–1753.
Işçimen, E. M., & Hayta, M. (2024). Proteins for analogue foods. In Ö. P. Can, M. GÖKsel SaraÇ, & D. Aslan TÜRker (Eds.), *Food analogues: Emerging methods and challenges* (pp. 115–144). Cham: Springer Nature Switzerland.
Jeong, H., Lee, J., Jo, Y.-J., & Choi, M.-J. (2023). Thermo-irreversible emulsion gels based on deacetylated konjac glucomannan and methylcellulose as animal fat analogs. *Food Hydrocolloids, 137*, Article 108407.
Jian, W., Siu, K.-C., & Wu, J.-Y. (2015). Effects of pH and temperature on colloidal properties and molecular characteristics of Konjac glucomannan. *Carbohydrate Polymers, 134*, 285–292.
Joyner, H. S. (2021). Nonlinear (Large-Amplitude oscillatory shear) rheological properties and their impact on food processing and quality. *Annual Review of Food Science and Technology, 12*, 591–609.
Kamer, D. D. A. (2024). Synergistic formulation approach for developing pea protein and guar gum enriched olive oil-in-water emulsion gels as solid fat substitutes: Formulation optimization, characterization, and molecular simulation. *International Journal of Biological Macromolecules, 257*, Article 128718.
Kerslake, E., Kemper, J. A., & Conroy, D. (2022). What's your beef with meat substitutes? Exploring barriers and facilitators for meat substitutes in omnivores, vegetarians, and vegans. *Appetite, 170*, Article 105864.
Kim, W., Wang, Y., Vongsvivut, J., Ye, Q., & Selomulya, C. (2023). On surface composition and stability of β-carotene microcapsules comprising pea/whey protein complexes by synchrotron-FTIR microspectroscopy. *Food Chemistry, 426*, Article 136565.
Klost, M., & Drusch, S. (2019). Structure formation and rheological properties of pea protein-based gels. *Food Hydrocolloids, 94*, 622–630.
Li, Y., Duan, M., Luo, Y., Liu, G., Liang, L., Liu, X., Zhang, J., Wen, C., & Xu, X. (2024). Study on emulsion-filled gels with oxidation stability: Structure, rheology, and baking applications. *Journal of Molecular Liquids, 412*, Article 125843.
Li, Y., Li, K., Guo, Y., Liu, Y., Zhao, G., Qiao, D., Jiang, F., & Zhang, B. (2024). Mechanism for the synergistic gelation of konjac glucomannan and κ-carrageenan. *International Journal of Biological Macromolecules, 277*, Article 134423.
Li, M. T., McClements, D. J., Liu, X. B., & Liu, F. G. (2020). Design principles of oil-in-water emulsions with functionalized interfaces: Mixed, multilayer, and covalent complex structures. *Comprehensive Reviews in Food Science and Food Safety, 19*(6), 3159–3190.
Li, X.-L., Meng, R., Xu, B.-C., Zhang, B., Cui, B., & Wu, Z.-Z. (2022). Function emulsion gels prepared with carrageenan and zein/carboxymethyl dextrin stabilized emulsion as a new fat replacer in sausages. *Food Chemistry, 389*, Article 133005.
Li, H., Wu, C., Yin, Z., Wu, J., Zhu, L., Gao, M., & Zhan, X. (2022). Emulsifying properties and bioavailability of clove essential oil pickering emulsions stabilized by octadecylaminated carboxymethyl curdlan. *International Journal of Biological Macromolecules, 216*, 629–642.
Lin, D., Kelly, A. L., & Miao, S. (2020). Preparation, structure-property relationships and applications of different emulsion gels: Bulk emulsion gels, emulsion gel particles, and fluid emulsion gels. *Trends in Food Science & Technology, 102*, 123–137.
Liu, S.-Y., Lei, H., Li, L.-Q., Liu, F., Li, L., & Yan, J.-K. (2023). Effects of direct addition of curdlan on the gelling characteristics of thermally induced soy protein isolate gels. *International Journal of Biological Macromolecules, 253*, Article 127092.
Liu, Z., Ren, X., Cheng, Y., Zhao, G., & Zhou, Y. (2021). Gelation mechanism of alkali induced heat-set konjac glucomannan gel. *Trends in Food Science & Technology, 116*, 244–254.
Lorenzo, G., Zaritzky, N., & Califano, A. (2018). Food gel emulsions: Structural characteristics and viscoelastic behavior. In T. J. Gutiérrez (Ed.), *Polymers for food applications* (pp. 481–507). Cham: Springer International Publishing.
Lu, Z., Wu, Z., Wu, K., Zhang, X., Zhang, Y., Zhang, J., Zhou, H., Fan, X., Zhou, L., Wang, R., & Luo, J. (2025). Impact of κ-carrageenan and locust bean gum on physicochemical properties and emulsion gel formation in casein-based systems. *Food Hydrocolloids, 169*, Article 111634.
Lu, W., Zheng, B., & Miao, S. (2018). Improved emulsion stability and modified nutrient release by structuring O/W emulsions using konjac glucomannan. *Food Hydrocolloids, 81*, 120–128.
Martins, A. J., Vicente, A. A., Cunha, R. L., & Cerqueira, M. A. (2018). Edible oleogels: An opportunity for fat replacement in foods. *Food & Function, 9*(2), 758–773.
Moghtadaei, M., Soltanizadeh, N., Goli, S. A. H., & Sharifimehr, S. (2021). Physicochemical properties of beef burger after partial incorporation of ethylcellulose oleogel instead of animal fat. *Journal of Food Science and Technology-Mysore, 58*(12), 4775–4784.
Naeli, M. H., Milani, J. M., Farmani, J., & Zargaraan, A. (2020). Development of innovative ethyl cellulose-hydroxypropyl methylcellulose biopolymer oleogels as low saturation fat replacers: Physical, rheological and microstructural characteristics. *International Journal of Biological Macromolecules, 156*, 792–804.
Nonoyama, T., & Gong, J. P. (2021). Tough double network hydrogel and its biomedical applications. *Annual Review of Chemical and Biomolecular Engineering, 12*, 393–410. Volume 12, 2021.
Öztürk-Kerimoglu, B., Kara, A., Urgu-Öztürk, M., & Serdaroglu, M. (2021). A new inverse olive oil emulsion plus carrot powder to replace animal fat in model meat batters. *Lwt-Food Science and Technology, 135*.
Rather, S. A., Masoodi, F. A., Akhter, R., Rather, J. A., Gani, A., Wani, S. M., & Malik, A. H. (2016). Application of guar–xanthan gum mixture as a partial fat replacer in meat emulsions. *Journal of Food Science and Technology, 53*(6), 2876–2886.
Ray, D. K., Sloat, L. L., Garcia, A. S., Davis, K. F., Ali, T., & Xie, W. (2022). Crop harvests for direct food use insufficient to meet the UN's food security goal. *Nature Food, 3*(5), 367–374.
Sha, L., & Xiong, Y. L. (2020). Plant protein-based alternatives of reconstructed meat: Science, technology, and challenges. *Trends in Food Science & Technology, 102*, 51–61.
Shao, P., Feng, J. R., Sun, P. L., Xiang, N., Lu, B. Y., & Qiu, D. (2020). Recent advances in improving stability of food emulsion by plant polysaccharides. *Food Research International, 137*.
Shi, Z., Chen, Z., & Meng, Z. (2023). Study on oil body emulsion gels stabilized by composited polysaccharides through microgel particles compaction and natural gelation. *Food Hydrocolloids, 135*, Article 108146.
Sogari, G., Caputo, V., Joshua Petterson, A., Mora, C., & Boukid, F. (2023). A sensory study on consumer valuation for plant-based meat alternatives: What is liked and disliked the most? *Food Research International, 169*, Article 112813.
Sridhar, K., Bouhallab, S., Croguennec, T., Renard, D., & Lechevalier, V. (2023). Recent trends in design of healthier plant-based alternatives: Nutritional profile, gastrointestinal digestion, and consumer perception. *Critical Reviews in Food Science and Nutrition, 63*(30), 10483–10498.
Su, L., Jing, L., Zeng, X., Chen, T., Liu, H., Kong, Y., Wang, X., Yang, X., Fu, C., Sun, J., & Huang, D. (2023). 3D-Printed prolamin scaffolds for cell-based meat culture. *Advanced Materials, 35*(2), Article 2207397.
United_Nations. (2015). *The UN sustainable development goals*. New York: United Nations.
Vallikkadan, M. S., Dhanapal, L., Dutta, S., Sivakamasundari, S. K., Moses, J. A., & Anandharamakrishnan, C. (2023). Meat alternatives: Evolution, structuring techniques, trends, and challenges. *Food Engineering Reviews, 15*(2), 329–359.
van Dijk, M., Morley, T., Rau, M. L., & Saghai, Y. (2021). A meta-analysis of projected global food demand and population at risk of hunger for the period 2010–2050. *Nature Food, 2*(7), 494–501.
Variyar, P. S., & Mishra, B. B. (2024). Chapter 15 - Flavor challenges in designing plant-based meat analogs: An overview. In G. A. Ravishankar, A. Ranga Rao, R. Tahergorabi, & A. Mohan (Eds.), *Handbook of plant-based meat analogs* (pp. 301–329). Academic Press.
Wang, Y., Kim, W., Naik, R. R., Spicer, P. T., & Selomulya, C. (2023). Tuning the pea protein gel network to mimic the heterogenous microstructure of animal protein. *Food Hydrocolloids, 140*.
Wang, Y., & Selomulya, C. (2022). Food rheology applications of large amplitude oscillation shear (LAOS). *Trends in Food Science & Technology, 127*, 221–244.
Wannasin, D., & McClements, D. J. (2023). Optimizing the appearance of plant-based foods: Impact of pigment and droplet characteristics on optical properties of model oil-in-water emulsions. *Food Biophysics, 18*(2), 289–301.
Wei, Y. Y., Guo, Y. L., Li, R. Q., Ma, A. Q., & Zhang, H. B. (2021). Rheological characterization of polysaccharide thickeners oriented for dysphagia management: Carboxymethylated curdlan, konjac glucomannan and their mixtures compared to xanthan gum. *Food Hydrocolloids, 110*.
Wen, Y., Che, Q. T., Kim, H. W., & Park, H. J. (2021). Potato starch altered the rheological, printing, and melting properties of 3D-printable fat analogs based on inulin emulsion-filled gels. *Carbohydrate Polymers, 269*.

Wijarnprecha, K., Fuhrmann, P., Gregson, C., Sillick, M., Sonwai, S., & Rousseau, D. (2022). Temperature-dependent properties of fat in adipose tissue from pork, beef and lamb. Part 2: Rheology and texture. *Food & Function, 13*(13), 7132–7143.

Xu, Q., Qi, B., Han, L., Wang, D., Zhang, S., Jiang, L., Xie, F., & Li, Y. (2021). Study on the gel properties, interactions, and pH stability of pea protein isolate emulsion gels as influenced by inulin. *Lwt, 137*, Article 110421.

Xu, Q., Wang, H., Ren, Y., Sun, M., Zhang, T., Li, H., & Liu, X. (2024). Functionality and application of emulsion gels in fat replacement strategies for dairy products. *Trends in Food Science & Technology, 152*, Article 104673.

Yang, X., Gong, T., Li, D., Li, A., Sun, L., & Guo, Y. (2019). Preparation of high viscoelastic emulsion gels based on the synergistic gelation mechanism of xanthan and konjac glucomannan. *Carbohydrate Polymers, 226*, Article 115278.

Yiu, C. C.-Y., Wang, Y., & Selomulya, C. (2025). Double network as a design paradigm for structuring emulsion gels in food. *Comprehensive Reviews in Food Science and Food Safety, 24*(3), Article e70201.

Younis, K., Ashfaq, A., Ahmad, A., Anjum, Z., & Yousuf, O. (2023). A critical review focusing the effect of ingredients on the textural properties of plant-based meat products. *Journal of Texture Studies, 54*(3), 365–382.

Zhang, C., Lu, M., Ai, C., Cao, H., Xiao, J., Imran, M., Chen, L., & Teng, H. (2023). Ultrasonic treatment combined with curdlan improves the gelation properties of low-salt Nemipterus virgatus surimi. *International Journal of Biological Macromolecules, 248*, Article 125899.

Zhang, Z. Y., Yang, Y. L., Tang, X. Z., Chen, Y. J., & You, Y. (2015). Chemical forces and water holding capacity study of heat-induced myofibrillar protein gel as affected by high pressure. *Food Chemistry, 188*, 111–118.

Zhao, X., Guo, R., Li, X., Wang, X., Zeng, L., Wen, X., & Huang, Q. (2023). Effect of oil-modified crosslinked starch as a new fat replacer on gel properties, water distribution, and microstructures of pork meat batter. *Food Chemistry, 409*, Article 135337.

Zhou, H., Vu, G., Gong, X., & McClements, D. J. (2022). Comparison of the cooking behaviors of meat and plant-based meat analogues: Appearance, texture, and fluid holding properties. *ACS Food Science & Technology, 2*(5), 844–851.

Zhu, J., He, Y., Wang, Y., & Cai, L.-H. (2024). Voxelated bioprinting of modular double-network bio-ink droplets. *Nature Communications, 15*(1), 5902.